AIP Conference Proceedings

RESEARCH ARTICLE | MAY 31 2018

Comparative microscopic dynamics in a room-temperature ionic liquid confined in carbon pores characterized by reversible and irreversible ion immobilization FREE

Eugene Mamontov ✉; Shannon M. Mahurin; Sheng Dai

Check for updates

AIP Conf. Proc. 1969, 020001 (2018)
https://doi.org/10.1063/1.5039290

View Online Export Citation

14 June 2024 16:49:10

APL Energy

Latest Articles Online!

Read Now

AIP Publishing

AIP Publishing

Comparative Microscopic Dynamics in a Room-Temperature Ionic Liquid Confined in Carbon Pores Characterized by Reversible and Irreversible Ion Immobilization

Eugene Mamontov[1, a)], Shannon M. Mahurin[2], Sheng Dai[2]

[1]*Chemical and Engineering Materials Division, Oak Ridge National Laboratory, Oak Ridge, Tennessee 37831, USA*
[2]*Chemical Sciences Division, Oak Ridge National Laboratory, Oak Ridge, Tennessee 37831, USA*

[a)]Corresponding author: mamontove@ornl.gov

Abstract. In search for the origin of irreversible ion immobilization under applied electric potential recently reported for a prototypical room-temperature ionic liquid electrolyte, [emim][Tf_2N], confined in 1.5 nm carbon pores, here we compare the microscopic dynamics of cations in [emim][Tf_2N] in the 1.5 nm and 6.7 nm carbon pores; in the latter, ion immobilization under applied electric potential is reversible. Using quasielastic neutron scattering, we find that the cation translational diffusivity is reasonably well defined on at least a nanometer length scale in the 6.7 nm pores, but not the 1.5 nm pores. Severely impeded microscopic dynamics of the confined electrolyte may be one of the factors differentiating the 1.5 nm pores from their larger counterparts and contributing to the irreversible immobilization of ions under applied electric potential.

14 June 2024 16:49:10

INTRODUCTION

A recently published study [1] showed that under applied electric potential, cations and anions of a prototypical room-temperature ionic liquid electrolyte, [emim][Tf_2N], exhibit irreversible immobilization on the walls of carbon pores of 1.5 nm, but not 6.7 nm, size. The measurements demonstrating irreversible immobilization were performed over several days and involved temperatures up to 350 K, thus suggesting, unexpectedly, that the first application of a positive or a negative electric potential across the carbon-electrolyte interface in sufficiently small pores may lead to a decoration of the carbon surface with ions that persists for long times and cannot be reversed by application of a potential of the opposite sign. On the other hand, application of an electric potential of the opposite sign showed reversibility of the carbon wall decoration for [emim][Tf_2N] in the 6.7 nm pores, as expected [1]. Because there was no obvious difference in the surface chemistry of the carbon in the two porous materials studied, here we explore a possibility that the difference in the microscopic dynamics (mobility) of the ions might contribute to the qualitatively different behavior of the electrolytes confined in the 1.5 nm and 6.7 nm carbon pores.

MATERIALS AND METHODS

The quasielastic neutron scattering (QENS) measurements carried out using the neutron backscattering spectrometer, BASIS [2], at the Spallation Neutron Source, ORNL, and the porous carbon materials measured using an *in situ* electrochemical cell were described in detail elsewhere [1]. Here we analyze the previously described data sets collected at 350 K at zero potential. Because of the large incoherent scattering cross-section of hydrogen compared to other elements, the QENS signals are predominantly sensitive to hydrogen-bearing cations of [emim][Tf_2N].

Proceedings of the Joint Conference on Quasielastic Neutron Scattering and the Workshop on Inelastic Neutron Spectrometers QENS/WINS 2016
AIP Conf. Proc. 1969, 020001-1–020001-6; https://doi.org/10.1063/1.5039290
Published by AIP Publishing. 978-0-7354-1676-5/$30.00

RESULTS AND DISCUSSION

Examples of the QENS data and fits at representative values of scattering momentum transfer of Q = 0.7 Å^{-1} (6.7 nm pores) and Q = 0.9 Å^{-1} (1.5 nm pores) are presented in Figure 1 along with the resolution function data.

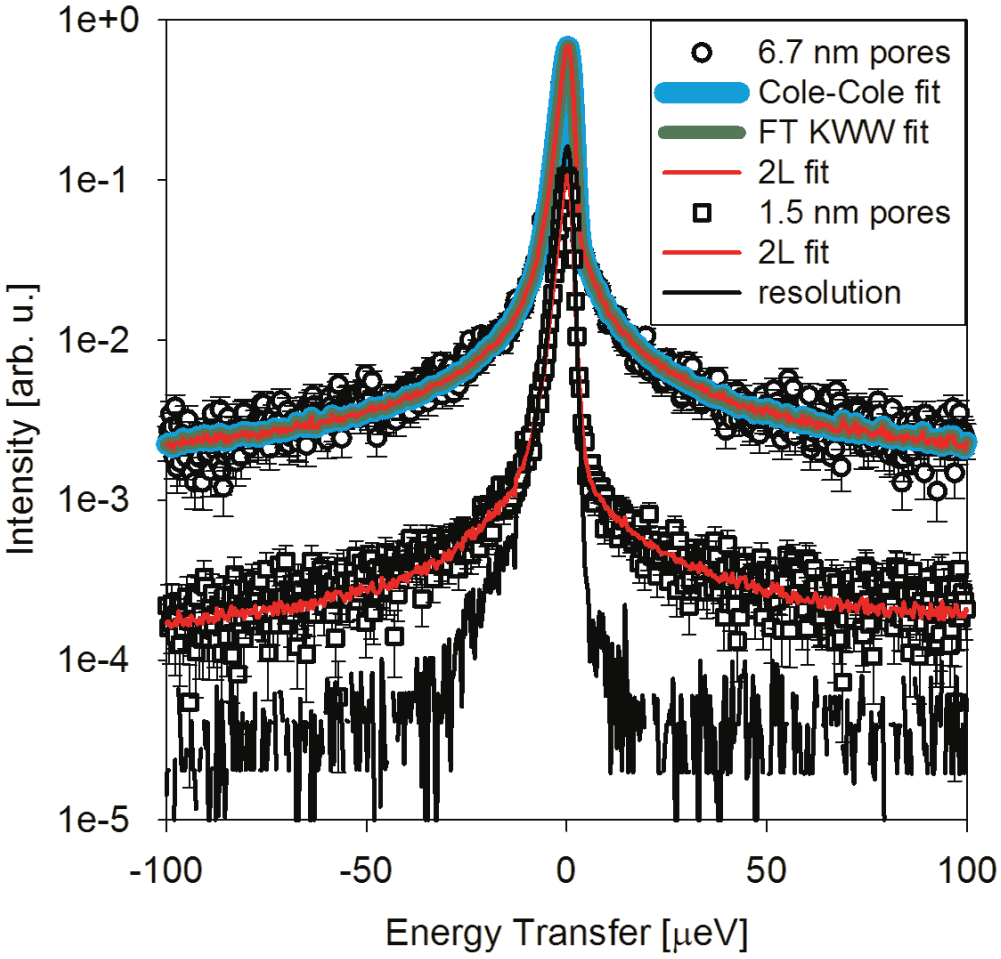

FIGURE 1. The QENS intensities and fits measured at Q = 0.7 Å^{-1} from [emim][Tf$_2$N] confined in the 6.7 nm carbon pores and Q = 0.9 Å^{-1} from [emim][Tf$_2$N] confined in the 1.5 nm carbon pores. The resolution function (at Q = 0.9 Å^{-1}) is also plotted.

In general, QENS data from confined fluids can be fitted using the following general expression:

$$I(Q,E) = \left[x(Q)\delta(E) + \left(1 - x(Q)\right)S(Q,E)\right] \otimes R(Q,E) + \left(C_1(Q)E + C_2(Q)\right) \quad (1)$$

Here a linear background is added to a convolution of the resolution function R(Q,E) with a superposition of a delta-function centered at zero energy transfer and a model scattering function, S(Q,E). The latter contains information in parametrized form that is relevant to the microscopic fluid dynamics. At first, we attempted to use two different model scattering functions; each of them accounted for the substantially non Debye-like character of ionic liquid relaxations in tight confinement (that is, the non-Lorentzian shape of the QENS signal). The first is the Cole-Cole scattering function, commonly used, e.g., in dielectric spectroscopy, and more recently adapted [3] to fit QENS data:

14 June 2024 16:49:10

$$S(Q,E) = \frac{1}{\pi E_0(Q)} \frac{(E/E_0(Q))^{-\alpha(Q)} \cos\frac{\pi\alpha(Q)}{2}}{1 + 2(E/E_0(Q))^{1-\alpha(Q)} \sin\frac{\pi\alpha(Q)}{2} + (E/E_0(Q))^{2(1-\alpha(Q))}} \quad (2)$$

When the "stretching" parameter, $0 < \alpha(Q) < 1$, equals zero, the Cole-Cole S(Q,E) becomes a Lorentzian. The parameter $E_0(Q)$ is analogous to the HWHM (half width at half maximum of a Lorentzian). The second is Fourier-transformed Kohlrausch-Williams-Watts ("stretched" exponential) function, commonly applied to substantially non Debye-like systems:

$$S(Q,E) = \int_0^\infty \exp\left[-\left(\frac{t}{\tau(Q)}\right)^{\beta(Q)}\right] \exp\left(i\frac{E}{\eta}t\right) dt \quad (3)$$

When the "stretching" parameter, $0 < \beta(Q) < 1$, equals one, the FT KWW S(Q,E) becomes a Lorentzian. The average relaxation time for this model scattering function is calculated as $\langle\tau(Q)\rangle = (\tau(Q)/\beta(Q))\Gamma(1/\beta(Q))$, where Γ is the gamma-function.

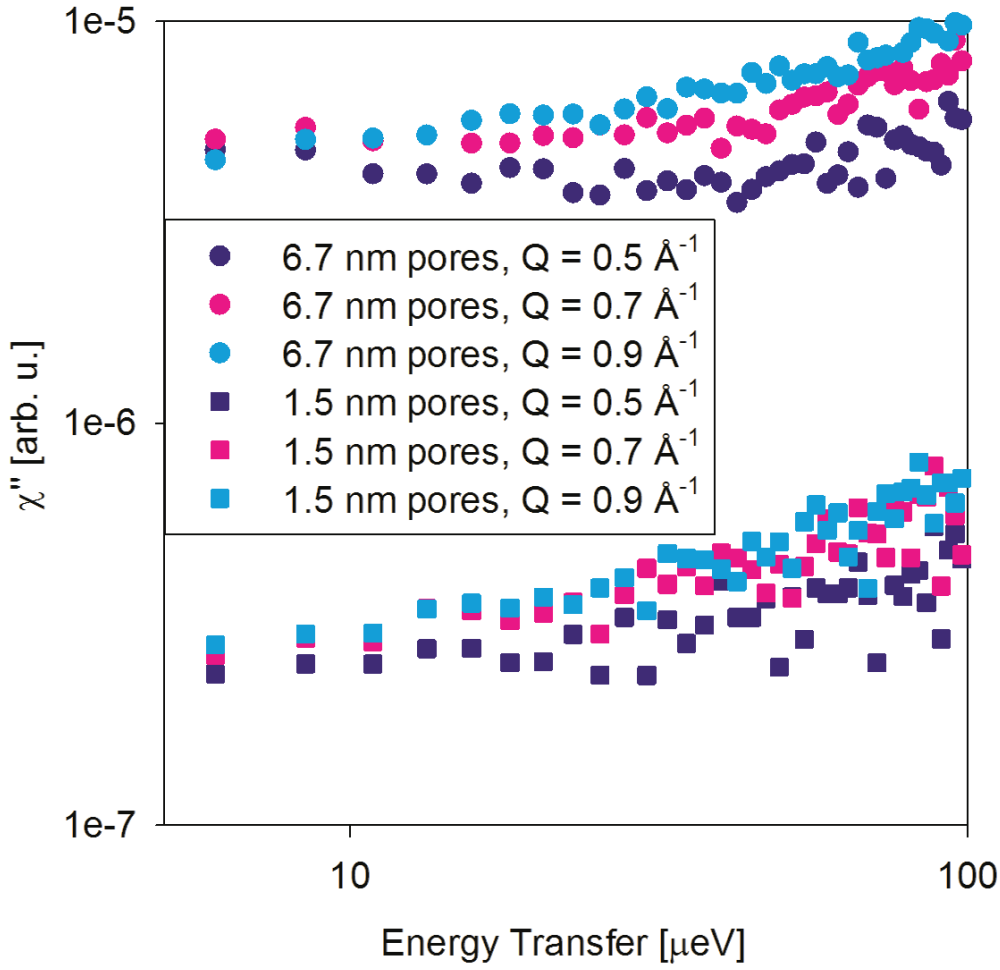

FIGURE 2. The dynamic susceptibilities calculated from the QENS scattering intensities for [emim][Tf_2N] confined in the 6.7 nm and 1.5 nm carbon pores.

14 June 2024 16:49:10

The QENS data were reduced using a standard binning scheme to obtain spectra at Q values of 0.3, 0.5, 0.7, 0.9, 1.1, 1.3, 1.5, 1.7, and 1.9 $Å^{-1}$. Even though both the 6.7 nm and 1.5 nm data sets exhibit broadening beyond the resolution signal, as one can readily see in Figure 1, the data fits converged only at Q = 0.5 $Å^{-1}$, Q = 0.7 $Å^{-1}$, and Q = 0.9 $Å^{-1}$ for the 6.7 nm data sets, and did not converge at any Q value for the 1.5 nm data sets, whether Cole-Cole or FT KWW model scattering function was used. The Cole-Cole fits of the 6.7 nm data yield E_0 = (3.5 ± 0.5) μeV, α = (0.36 ± 0.05); E_0 = (8.5 ± 0.7) μeV, α = (0.36 ± 0.05); E_0 = (17.9 ± 4.3) μeV, α = (0.42 ± 0.06), for 0.5 $Å^{-1}$, 0.7 $Å^{-1}$, 0.9 $Å^{-1}$, respectively. The FT KWW fits of the 6.7 nm data yield τ = (148 ± 15) ps, β = (0.56 ± 0.05), $1/\langle\tau\rangle$ = (2.7 ± 0.5) μeV; τ = (60 ± 6) ps, β = (0.51 ± 0.05), $1/\langle\tau\rangle$ = (5.6 ± 1.2) μeV; τ = (16 ± 10) ps, β = (0.33 ± 0.07), $1/\langle\tau\rangle$ = (6.7 ± 5.5) μeV, for 0.5 $Å^{-1}$, 0.7 $Å^{-1}$, 0.9 $Å^{-1}$, respectively.

The case of [emim][Tf_2N] in the 1.5 nm pores may be analogous to the previously studied [emim][TFSI] confined in even smaller pores of carbide-derived-carbons, where no explicit relaxation times could be extracted because of the unusual spectral shape of the relaxation signal indicative of the completely localized (non-translational) cation dynamics [4]. Nevertheless, it is instructive to see what specific features in the scattering signal render the data quantitatively analyzable (albeit only at a few Q values) for the 6.7 nm, but not the 1.5 nm, data set. To this end, Figure 2 shows the dynamic susceptibilities, calculated from the scattering intensities as $\chi''(Q,E) = I(Q,E)/n_b(E)$, where $n_b(E)$ is the thermal Bose factor, at Q = 0.5 $Å^{-1}$, Q = 0.7 $Å^{-1}$, and Q = 0.9 $Å^{-1}$. In general, there are no well-defined peaks that would be clearly indicative of specific relaxation processes within the experiment window, and the susceptibility spectra are dominated by the tail that gradually increases in intensity (beyond the maximum accessible range of energy transfer) due to fast localized dynamics processes. Nevertheless, unlike for the 1.5 nm data set, the low-energy part of the spectra for the 6.7 nm data set may exhibit just enough intensity at these Q values for the low-energy modes to be analyzable with fits using Equations (1-2) or (1-3).

In view of the limited success of the "stretched" model scattering functions in the 6.7 nm data sets fits and their failure in the 1.5 nm data sets fits, we then resorted to the generic two-Lorentzian model scattering function:

$$S(Q,E) = p(Q)\frac{1}{\pi}\frac{\Gamma_1(Q)}{\Gamma_1(Q)^2 + E^2} + (1 - p(Q))\frac{1}{\pi}\frac{\Gamma_2(Q)}{\Gamma_2(Q)^2 + E^2} \quad (4)$$

For bulk room-temperature ionic liquids, this model scattering function is actually preferred to the "stretched" model scattering function [5]. The two-component model describes the long-range translational and localized dynamic components [5]. The lack of well-defined peaks in the susceptibility spectra in Figure 2 indicates that the use of Equations (1-4) for our systems may not be intuitive, and we attempt it only because the "stretched" relaxation functions have not been quite satisfactory. We have found that data fits using Equations (1-4) converged at Q = 0.5 $Å^{-1}$ and Q = 0.7 $Å^{-1}$ for the 6.7 nm data sets and Q = 0.9 $Å^{-1}$ for the 1.5 nm data sets. For the 6.7 nm data, we obtain Γ_1 = (2.4 ± 0.4) μeV, Γ_2 = (15.6 ± 2.2) μeV, p = (0.64 ± 0.03) at 0.5 $Å^{-1}$ and Γ_1 = (4.6 ± 0.4) μeV, Γ_2 = (30.4 ± 5.1) μeV, p = (0.61 ± 0.03) at 0.7 $Å^{-1}$. For the single Q value of 0.9 $Å^{-1}$ that could be fitted for the 1.5 nm data, we obtain Γ_1 = (0.7 ± 0.3) μeV, Γ_2 = (22.4 ± 2.6) μeV, p = (0.65 ± 0.06). It is the narrow component, Γ_1, which accounts for the long-range translational diffusivity in the two-component model scattering function [5].

The QENS broadening values (representing the inverse average relaxation times) are presented in Figure 3. The different model scattering functions give rise to the very similar data fits (as one can see in Figure 1), yet the resulting average relaxation times are somewhat different because of the way the average value of a "stretched" time distribution is calculated in Cole-Cole and FT KWW models.

Regardless of the exact values, which are somewhat model-dependent, the data points with smaller error bars (at 0.5 and 0.7 $Å^{-1}$) are indicative of the Q-dependent dynamic process for the 6.7 nm data sets that could be considered translational diffusion, at least on a nanometer length scale. As such, this process could be fitted with a DQ^2 law to obtain the effective translational diffusion coefficient, D, as shown in Figure 3. For comparison, a translational diffusion coefficient of ca. $4*10^{-10}$ m^2/s at 350 K was measured by QENS for [bmim][Tf_2N] confined in carbon with 8.8 nm pore size [6]. Concerning the 1.5 nm data sets, only a qualitative conclusion can be reached. Even if the dynamics of cations in [emim][Tf_2N] could be considered translational on a nanometer length scale, the corresponding diffusion coefficient that could be obtained from the (0.7 ± 0.3) μeV broadening at Q = 0.9 $Å^{-1}$ would be at least an order of magnitude smaller than that for the 6.7 nm data sets. More likely, it is the localized (non-translational) character of the cation dynamics in the 1.5 nm pores that precludes quantitative analysis of QENS broadening at lower Q values, because for localized processes the intensity (but not the width) of the broadening signal increases with Q.

14 June 2024 16:49:10

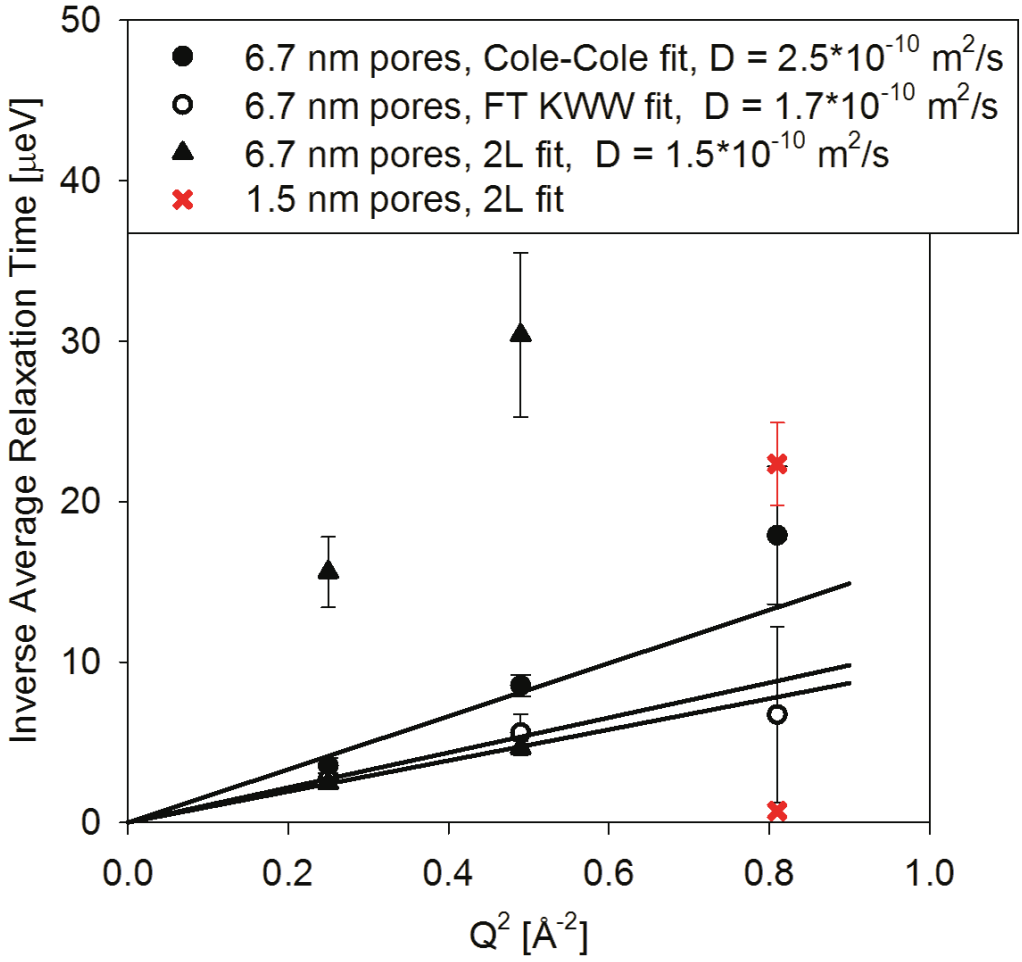

FIGURE 3. The QENS broadening parameters (symbols) and the corresponding DQ^2 fits (solid lines) used to obtain translational diffusion coefficient, D, for the cations in [emim][Tf_2N] confined in 6.7 nm carbon pores. Also shown as red crosses are the broadening parameters obtained at a single Q value for the cations in [emim][Tf_2N] confined in 1.5 nm carbon pores.

Our QENS data analysis was beset with serious difficulties. Even in the best case scenario, QENS data from bulk and especially confined room-temperature ionic liquids are typically hard to analyze beyond ca. Q = 1.3 $Å^{-1}$ [6-8] due to the rapidly increasing coherent scattering associated with approaching the structure factor maximum. Measurements at the lowest Q values, such as 0.3 $Å^{-1}$, are oftentimes affected by the strong tail of the small-angle coherent scattering signal from powder samples. The useful Q-range could be further limited in the current experiment by the geometry of the custom-designed electrochemical cell [1], which might affect neutrons scattered in the directions close to the cell plane. These factors might explain why the overall analyzable Q range was limited to values below 0.9 $Å^{-1}$. However, the difference between the 6.7 nm data sets (mostly analyzable) and 1.5 nm data sets (hardly analyzable) must originate from the intrinsic difference in the respective scattering signals. As we have discussed above, the peaks in the dynamic susceptibility spectra (Figure 2) are not well-defined for either pore size, but the difference in the QENS signal intensity (by an order of magnitude) may render the 1.5 nm data sets difficult to analyze quantitatively. The future work will likely involve measuring the 1.5 nm sample using more favorable annular cell geometry and the powdered carbon material loaded with the ionic liquid ex situ. Nevertheless, the data analysis might still prove difficult, largely because of the overwhelmingly strong elastic scattering from the 1.5 nm sample due to the immobilized cations [1]. The susceptibility spectra for the 1.5 nm data sets presented in Figure 2 exhibit relatively weak intensity not because of the insufficient amount of the ionic liquid in the sample, but due to

14 June 2024 16:49:10

the dominant elastic scattering by this ionic liquid. Most of the ions in the sample are immobile on the nano-second resolution time scale of the BASIS, thus contributing to the elastic line and making the quasileastic signal weak and difficult to analyze. Raising measurement temperature in order to decrease the fraction of the immobilized ions might have a limited potential, because the currently used temperature of 350 K is already rather high. Compared to backscattering, only neutron spin-echo could offer decisively better resolution, thus potentially increasing the fraction of ions perceived as mobile on the resolution time scale of the experiment. However, besides general difficulties encountered in neutron spin-echo measurements of incoherently scattering species, such measurements performed in the time space are even less efficient in separating dynamic signal from the elastic background compared to the measurements performed in the energy space (such as backscattering). Therefore, ionic liquids confined in the 1.5 nm pore sample may exemplify a system that is not readily amenable to experimental analysis by neutron scattering techniques and would be analyzed more efficiently using molecular dynamics simulations. With sufficiently long simulations times, there might be a possibility to resolve the ion dynamics that cannot be resolved in the experiment. However, certain types of microscopic dynamics of confined ionic liquids, such as, e.g., logarithmic decay as a function of the relaxation time [4], may prove difficult to analyze qualitatively regardless of the limitations imposed by the resolution of the probe, in either experiments or simulations.

CONCLUSION

A room-temperature ionic liquid, [emim][Tf_2N], exhibits significant microscopic dynamics when confined in carbon pores of 6.7 nm and 1.5 nm size, as evidenced by quasielastic neutron scattering experiments carried out at 350 K. However, this dynamics is dominated by fast localized processes, whereas the translational diffusivity, characterized by the center-of-mass mobility, is suppressed to the extent that it is hardly measurable in the 1.5 nm pores, even on a nanometer length scale. We propose that the seemingly qualitative difference between the 6.7 nm and 1.5 nm pores (measurable translational diffusivity vs. hardly detectable diffusivity) might be a factor profoundly contributing to the recently reported irreversible ion immobilization under applied electric potential in the 1.5 nm, but not 6.7 nm, carbon pores.

14 June 2024 16:49:10

ACKNOWLEDGMENTS

This work was supported as part of the Fluid Interface Reactions, Structures and Transport (FIRST) Center, an Energy Frontier Research Center funded by the U.S. Department of Energy, Office of Science, Office of Basic Energy Sciences. The neutron scattering experiments at Oak Ridge National Laboratory's (ORNL) Spallation Neutron Source were supported by the Scientific User Facilities Division, Office of Basic Energy Sciences, U.S. Department of Energy. This manuscript has been authored by UT-Battelle, LLC under Contract No. DE-AC05-00OR22725 with the U.S. Department of Energy. The United States Government retains and the publisher, by accepting the article for publication, acknowledges that the United States Government retains a non-exclusive, paid-up, irrevocable, world-wide license to publish or reproduce the published form of this manuscript, or allow others to do so, for United States Government purposes. The Department of Energy will provide public access to these results of federally sponsored research in accordance with the DOE Public Access Plan (http://energy.gov/downloads/doe-public-access-plan).

REFERENCES

1. S. M. Mahurin, E. Mamontov, M. W. Thompson, P. Zhang, C. H. Turner, P. T. Cummings, and S. Dai, Appl. Phys. Letters **109**, 143111 (2016).
2. E. Mamontov and K. W. Herwig, Rev. Sci. Instr. **82**, 085109 (2011).
3. E. Mamontov and H. O'Neill, Biochim. Biophys. Acta **1861**, 3513 (2017).
4. B. Dyatkin, E. Mamontov, K. M. Cook, and Y. Gogotsi, Progress in Natural Science: Materials International **25**, 631 (2015).
5. E. Mamontov, H. Luo, and S. Dai, J. Phys. Chem. B **113**, 159 (2009).
6. S. M. Chathoth, E. Mamontov, S. Dai, X. Wang, P. F. Fulvio, and D. J. Wesolowski, EPL **97**, 66004 (2012).
7. S. M. Chathoth, E. Mamontov, P. F. Fulvio, X. Wang, G. A. Baker, S. Dai, and D. J. Wesolowski, EPL **102**, 16004 (2013).
8. E. Mamontov, G. A. Baker, H. Luo, and S. Dai, ChemPhysChem **12**, 944 (2011).